

OPTICAL LOW ANGLE PASS FILTER FOR HIGH RESOLUTION ROBUST PHOTOPLETHYSMOGRAPHY MONITOR

Chan-Sol Hwang, Sung-Pyo Yang, Jung-Woo Park, and Ki-Hun Jeong*

Department of Bio and Brain Engineering, KAIST, Daejeon, Republic of Korea

ABSTRACT

We report an optical low angle pass filter (OLAPF) to enhance the signal-to-noise ratio (SNR) using the slanted mirror structure which angle selectively block the light in photoplethysmography (PPG). The reflectance type PPG signal is using the reflected light from the capillary as a signal distorted by the scattered light. The OLAPF can block the light, which scattered by the human tissue, losing their directionality, while transmit the light which has directionality. The device can be used for smart watch, smart phone, and NIRS to get the signal from the underneath of the biological tissue.

KEYWORDS

Photoplethysmography, Optical Filter

INTRODUCTION

The photoplethysmography (PPG) sensor has been widely used for monitoring the human health status such as heart rate, blood oxygen saturation, and vascular activity can be estimated by analyzing the wave form and the cycle of the PPG signal [1, 2]. The PPG sensor can be divided into two types for using transmitted or reflected light [3]. The transmittance type using the transmitted light through the human organ such as ear lobes and fingertip has a robust to the noise from the outside of the human tissue and good signal quality, but this type has limited measurement site which made hard to use for wearable device such as smart watch and smart phone. While, the reflectance type PPG sensor has unlimited measurement site, but the signal is easily distorted by the noise. In wearable device such as smart phone and smart watch, the reflectance type sensor is widely used to measure the signal because of the advantage of the unlimited measurement site.

The wave form of the PPG signal is important to get parameters, which represent the human vascular activity and a human verification biometric variables [4]. The PPG signal has parameters such as diastolic peak, systolic peak, pulse interval, interval between systolic and diastolic peak, pulse width, and the inflection point area ration. However, the low SNR of conventional reflectance type PPG monitor hinders identifying the health status based on the PPG wave form losing the parameters except the systolic peak and pulse interval. The previous researches have been only focused on reducing the noise from the outside of the human tissue increasing the number of electrical device such as photodetector (PD), LED, and accelerometer or developing the signal processing techniques, which result in the high electrical power consumption and high calculation complexity hard to apply for the real-time processing [5–8].

CONCEPT AND PRINCIPLES

In this work, we represent the OLAPF blocking the scattered light from the inside of the human tissue, which is

a noise in the PPG signal. The light flux under the tissue is described as a “banana patterns” [9]. The light under the human tissue is losing their directionality by scattering in the human tissue. Figure. 1 (a) shows the schematic diagram of the light path under the human tissue. The partial reflected light, which has a low intensity detected as a noise, from the blood vessel is losing their directionality until reach to the PD. We design the OLAPF accepting the light which has an incident angle same as the LED’s emitting angle and blocking the other lights.

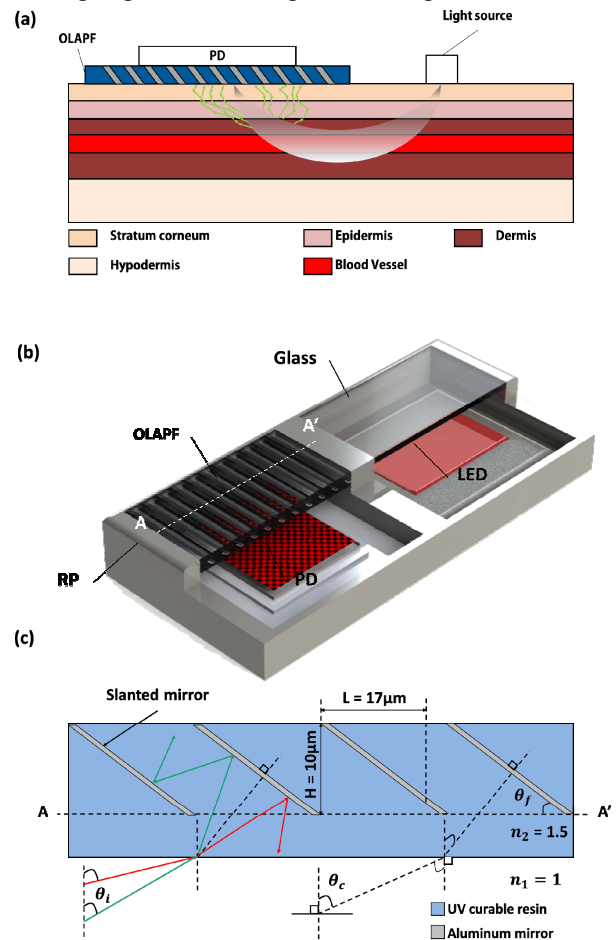


Figure 1:(a) The light is scattered by the human tissue and the scattered light is losing their directionality. (b) A schematic diagram of the PPG module with optical low angle pass filter (OLAPF). The OLAPF is on the PD to block the scattered light as a noise in the PPG signal. The mirror is on the LED to protect the electrical device from the shock. (c) The green arrow which has lower incident angle (θ_i) than the cut-off angle (θ_c) is transmitted light and red arrow which has higher θ_i than θ_c is blocked light filtered by the OLAPF.

Figure. 1 (b) shows a schematic diagram of the PPG module with the OLAPF which applied to the conventional PPG monitor. The OLAPF is put on the PD for blocking the scattered light and protecting electrical device. Figure.

1 (c) shows the design parameters of the OLAPF that the prism height is $10\ \mu\text{m}$ and the length is $17\ \mu\text{m}$ to make the $30\ \text{deg}$ of the filter angle (θ_f). Our target transmittance of the OLAPF is 0.5 when the incident angle is $0\ \text{deg}$. We assume that the light which has an incident angle same as the LED's emitting angle is considered as a PPG signal and the other lights are the noise in the PPG signal. We determine the transmittance when the incident angle is $0\ \text{deg}$ changing θ_f .

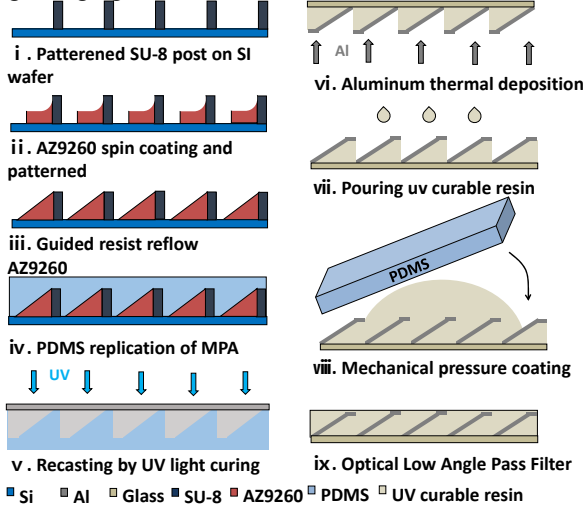


Figure 2: Fabrication procedure of the optical low angle pass filter (OLAPF). First, Fabrication of the micro prism array (MPA) using guided-resist reflow method. Patterning SU-8 post on Si wafer to support the AZ9260 as thermoplastic photoresist. Heating Si wafer to form the inclined plane of the MPA which has the $30\ \text{deg}$ of the prism angle. Replication of the MPA structure using Polydimethylsiloxane (PDMS) for uv-curable resin replication. The cavity between the prism post and the prism is filled by the uv-curable resin as a index matching material. Using PDMS slab to flat the top of the OLAPF in last step.

FABRICATION OF OPTICAL LOW ANGLE PASS FILTER

The microfabrication procedures of OLAPF are described in Fig. 2. The fabrication procedures start with the fabrication of the micro prism array (MPA) using geometry-guided resist reflow method[10]. First, patterning the SU-8 post as a thermoset resist on a Si wafer. The post height is $10\ \mu\text{m}$ and the width is $3\ \mu\text{m}$. AZ9260 was spin coated and patterned as a thermoplastic to make the MPA on a large scale. Heating the wafer to reflow the AZ9260 to form the MPA. Figure. 3 (a-b) are the SEM images that the MPA, which has a $30\ \text{deg}$ filter angle (θ_f) is successfully fabricated in a large scale on Si wafer. The MPA structure of the uv-curable resin is transferred to the transparent cover glass by soft lithography using the Polydimethylsiloxane (PDMS) replicated by the MPA. Aluminum mirror was formed on the MPA's inclined plane using thermal evaporation. The thickness of the mirror is $500\ \text{nm}$ to form the fully opaque mirror. The uv-curable resin is poured on the MPA to fill the cavity between the MPA for index matching between the post and air. And the mechanical pressure was applied the uv-curable resin using the PDMS slab to flat the top of the OLAPF. Figure. 3 (c) is

the optical image of the OLAPF, which incident angle of the light over the cut-off angle (θ_c) blocked the image "KAIST". Figure. 3 (d) shows transmitted the image "KAIST" when the incident angle of the light is less than θ_c .

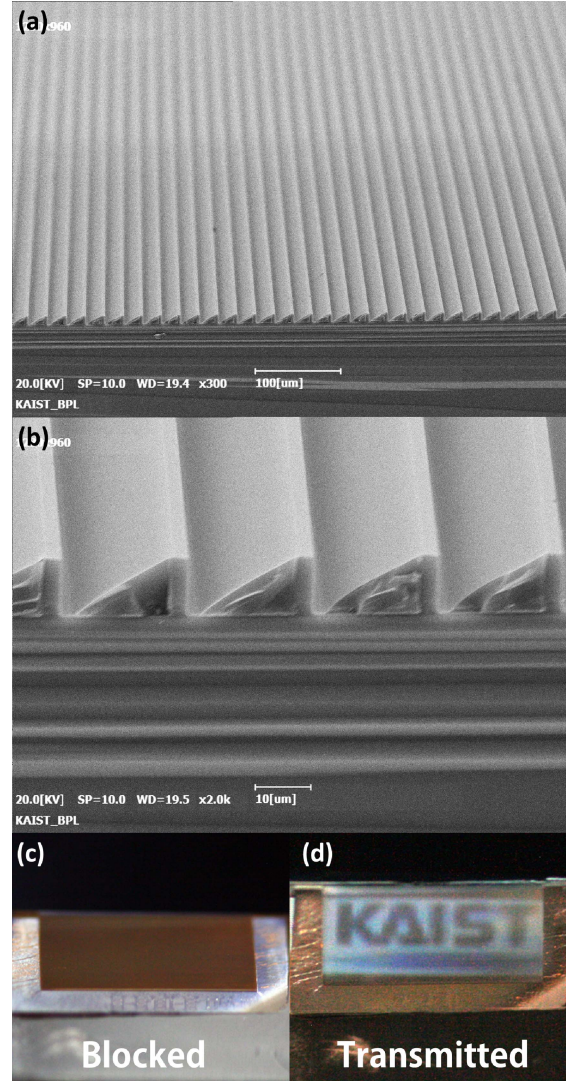


Figure 3: (a) The SEM image of oblique angle view of the micro prism array (MPA). MPA is fabricated in a large area on Si wafer. (b) The MPA is fabricated which has $10\ \mu\text{m}$ post height, $3\ \mu\text{m}$ width and $17\ \mu\text{m}$ prism width. The filter angle (θ_f) is $30\ \text{deg}$. The gap between the prism post and prism is $2\ \mu\text{m}$. (c) The OLAPF when incident angle is over cut-off angle (θ_c) is blocked the image "KAIST". (d) The OLAPF when incident angle is less than θ_c is transmitted the image "KAIST"

TRANSMITTANCE OF OPTICAL LOW ANGLE PASS FILTER

Figure. 4 (a) shows the experimental set-up of the OLAPF, which attached on the integrating sphere to measure the transmittance of the OLAPF. The rotation angle of the integrating sphere is $-80\ \text{deg}$ to $80\ \text{deg}$ and the light source is 533nm laser. Numerical analysis was conducted by using "ASAP 2015 V1 SP4". In this simulation, modeling the prism array without post width and the gap between the post and micro prism for ideal

condition of the MPA. The reflectance of aluminum is negligibly small in simulation. Figure 4 (b) shows the results of the simulation and experiment of the OLAPF. The mismatch between the simulation and experiment result is occurred by the post width and the gap in fabricated OLAPF. The transmittance of the OLAPF is not zero, when the incident angle is over the cut-off angle of the OLAPF caused by the diffraction on the edge of the aluminum mirror.

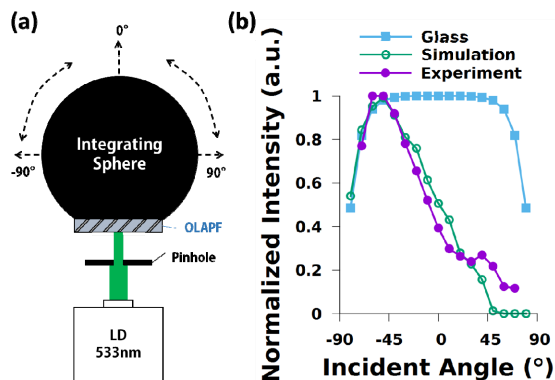


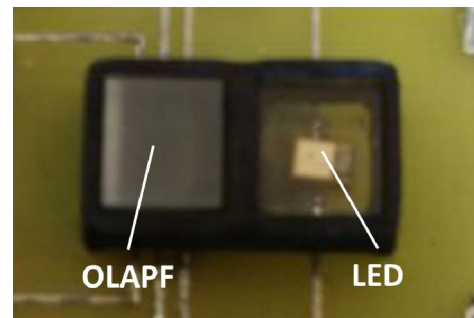
Figure 4: The transmittance of the OLAPF. (a) The experiment set-up to measure the transmittance of the OLAPF attached on the integrating sphere changing the incident angle of the light. The rotation angle is -80 deg to 80 deg. The pinhole is reduce the beam spot size on the OLAPF. (b) The transmittance of the OLAPF measured by simulation and experiment. The mismatch between simulation and experiment is occurred by the post width and gap between prism post and micro prism of the OLAPF. Over the cut-off angle of the OLAPF, the experiment result is not zero caused by the diffraction on the edge of the aluminum mirror.

PHOTOPLETHYSMOGRAPHY MONITOR WITH OPTICAL LOW ANGLE PASS FILTER

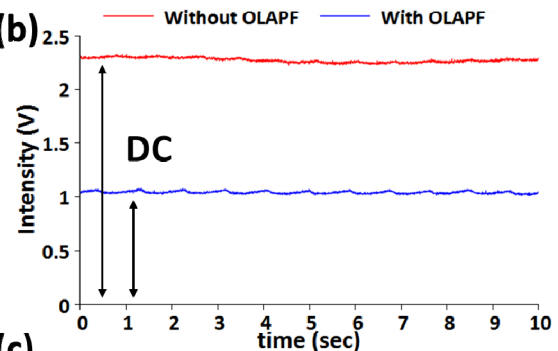
Figure 5 (a) shows the PPG monitor with OLAPF. The electrical devices such as LED and PD are soldered on the printed circuit board (PCB). The measured site of the PPG signal is forearm to compare the PPG signal with and without OLAPF. The intensity of the LED and sensitivity of the PD is the same in both cases. Figure 5 (b) shows the raw data of the PPG signal with noise, which reduced the DC noise by the OLAPF. The noise can be categorized by two types. One is low frequency noise which has the lower frequency than the signal, and the other is the high frequency noise which has the higher frequency than the signal. The low DC noise means that the PPG signal with OLAPF is more stable and robust. Figure 5 (c) shows the normalized intensity of the OLAPF. In this graph, the high frequency noise in both cases is similar to each other. The high frequency noise is not affect to the diastolic peak of the PPG signal which distributed on the bandwidth over the diastolic peak. The signal-to-noise ratio (SNR) is the ratio between the signal power and the noise power. According to these results, the SNR of the PPG signal with OLAPF is much higher than without OLAPF. In PPG signal, the low frequency noise distorts the wave form which crushed the diastolic peak. Using the OLAPF, we can get more stable

and robust PPG signal more stable and robust signal.

(a)



(b)



(c)

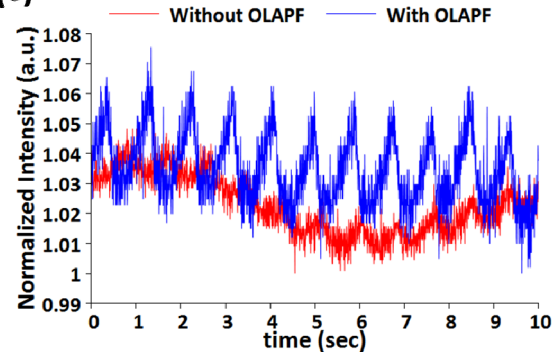


Figure 5: The PPG monitor with OLAPF. (a) The LED and PD are soldered on the PCB. The OLAPF is on the PD to block the scattered light from the human tissue and protect the PD from the shock. (b) Raw data with and without OLAPF shows that the low frequency noise is reduced by OLAPF. The low frequency noise affects to the stability and the wave form of the signal to lose their diastolic peak. (c) The normalized data with and without OLAPF shows that the high frequency noise of the PPG signal is similar to both cases. But the fluctuation of the signal with OLAPF is much stable than without OLAPF. It means that the low frequency SNR with OLAPF is better than without OLAPF.

CONCLUSION

In summary, the optical low angle pass filter to block the scattered light from the human tissue for enhancing the SNR of the PPG signal to preserve the diastolic peak of the signal was designed, fabricated and characterized. A transmittance of the OLAPF is measured by the integrating sphere to rotate for changing the incident angle of the light. The transmittance of the OLAPF shows the light which has the angle lower than cut-off angle is transmitted through the OLAPF. We made the conventional PPG monitor with and without OLAPF soldered PD and LED on the PCB.

The measured signal shows that the signal with OLAPF has higher low frequency SNR than without OLAPF. It means that the stability of the diastolic peak in PPG signal is enhanced by the OLAPF. The OLAPF is applied conventional PPG monitor replaced the transparent cover such as glass to protect the PD in the monitor. And it can be used for the electrical device which can be used for detecting signal from the under the human skin such as NIRS. Moreover, if we develop the computational imaging method using the OLAPF, we can be imaging the blood vessel under the human tissue.

ACKNOWLEDGEMENTS

This work was supported by the National Research Foundation of Korea (2016013061, 2016924609, 2016919193), funded by the Ministry of Science, ICT & Future Planning, and a grant of the Korean Health Technology R&D Project through the Korea Health Industry Development Institute (KHIDI), funded by Ministry of Health & Welfare, Republic of Korea (grant number: HI13C2181, HI16C1111).

REFERENCES

- [1] J. Allen, "Photoplethysmography and its application in clinical physiological measurement," *Physiological Measurement*, vol. 28, no. 3, p. R1, 2007.
- [2] P. J. Chowienzyk, R. P. Kelly, H. MacCallum, S. C. Millasseau, T. L. . Andersson, R. G. Gosling, J. M. Ritter, and E. E. Änggård, "Photoplethysmographic assessment of pulse wave reflection Blunted response to endothelium-dependent beta2-adrenergic vasodilation in type II diabetes mellitus," *Journal of the American College of Cardiology*, vol. 34, no. 7, pp. 2007–2014, 1999.
- [3] T. Tamura, Y. Maeda, M. Sekine, and M. Yoshida, "Wearable Photoplethysmographic Sensors—Past and Present," *Electronics*, vol. 3, no. 2, p. 282, 2014.
- [4] Y. Y. Gu, Y. Zhang, and Y. T. Zhang, "A novel biometric approach in human verification by photoplethysmographic signals," in *Information Technology Applications in Biomedicine, 2003. 4th International IEEE EMBS Special Topic Conference on*, 2003, pp. 13–14.
- [5] M. R. Ram, K. V. Madhav, E. H. Krishna, N. R. Komalla, and K. A. Reddy, "A Novel Approach for Motion Artifact Reduction in PPG Signals Based on AS-LMS Adaptive Filter," *IEEE Transactions on Instrumentation and Measurement*, vol. 61, no. 5, pp. 1445–1457, May 2012.
- [6] R. W. C. G. R. Wijshoff, M. Mischi, J. Veen, A. M. van der Lee, and R. M. Aarts, "Reducing motion artifacts in photoplethysmograms by using relative sensor motion: phantom study," *Journal of Biomedical Optics*, vol. 17, no. 11, pp. 117007–117007, 2012.
- [7] M. J. Hayes and P. R. Smith, "Artifact reduction in photoplethysmography," *Applied Optics*, vol. 37, no. 31, pp. 7437–7446, Nov. 1998.
- [8] H. H. Asada, H.-H. Jiang, and P. Gibbs, "Active noise cancellation using MEMS accelerometers for motion-tolerant wearable bio-sensors," in *Engineering in Medicine and Biology Society, 2004. IEMBS '04. 26th Annual International Conference of the IEEE*, 2004, vol. 1, pp. 2157–2160.
- [9] T. Durduran, R. Choe, W. B. Baker, and A. G. Yodh, "Diffuse optics for tissue monitoring and tomography," *Reports on Progress in Physics*, vol. 73, no. 7, p. 076701, 2010.
- [10] J.-J. Kim, S.-P. Yang, D. Keum, and K.-H. Jeong, "Asymmetric optical microstructures driven by geometry-guided resist reflow," *Opt. Express*, vol. 22, no. 18, pp. 22089–22094, Sep. 2014.

CONTACT

*Ki-Hun Jeong, tel: +82-42-350-4323; kjeong@kaist.ac.kr